LA-11060-MS

Los Alamos National Laboratory is operated by the University of California for the United States Department of Energy under contract W-7405-ENG-36

Electromagnetic Pulse (EMP) from Surface Bursts

Los Alamos National Laboratory
Los Alamos, New Mexico 87545

LA-11060-MS

UC-11
Issued: August 1987

Electromagnetic Pulse (EMP) from Surface Bursts

Tim Murphy

Los Alamos National Laboratory
Los Alamos, New Mexico 87545

ELECTROMAGNETIC PULSE (EMP) FROM SURFACE BURSTS

by

Tim Murphy

ABSTRACT

We present a simple analytic model to estimate the electromagnetic pulse (EMP) produced by the asymmetric Compton current distribution coming from a nuclear explosion on or near the earth's surface. The model does not include the effect of return currents in the air and ground and so is most appropriate for high-frequency EMP. It can be used to calculate the signal seen at a remote observation point at any angle above the surface of the earth. We find that the high-frequency signal from this effect is comparable with or larger than the geomagnetic turning signal from a surface burst and must therefore be considered in attempting to interpret existing EMP data.

I. INTRODUCTION

One effect produced by an above-ground nuclear explosion is a very fast electromagnetic pulse (EMP) due to the generation of electron Compton currents in the atmosphere by gamma-ray emissions from the nuclear device. The pulse is broadband, with frequencies ranging from a few kilohertz up to hundreds of megahertz. The bulk of the energy is at the low-frequency end of the spectrum, but there is enough energy at the high end to pose a threat to electronic equipment. Therefore the problem of how this pulse is generated has been the subject of considerable study. Because of the rapid risetime and large amplitude of the gamma-ray source, the amount of energy in such a pulse is potentially very large, but in order for it to be radiated efficiently, there must be a source of asymmetry in the Compton current system. One such source is geomagnetic turning, where the electrons are accelerated in a coherent fashion as they precess about the magnetic field lines of the earth. Because the earth's field is weak, this effect does not produce a large asymmetry, but for most atmospheric explosions it is the only source of EMP and has therefore been studied extensively. For high-altitude bursts the very large mean free path of the electrons and the enormous volume of the region in which the gamma rays are deposited combine to produce a significant EMP signal even though the asymmetry is small.

For explosions very near the ground, the earth itself is another source of asymmetry. Gamma rays emitted downward are intercepted by the earth's surface and do not produce large Compton currents, while those going upward do so. The degree of the resulting asymmetry is strongly dependent on the location from which the explosion is observed, and the field strengths produced can be larger than those due to the geomagnetic turning effect. Previous work in this area has concentrated on the EMP seen on the ground at a point fairly close to

the source and has relied on elaborate computer models to include the effect of ground conductivity, inducted air conductivity, and air chemistry. In this report we present a simple analytic calculation to estimate the EMP signal seen by a remote observer at any angle above the ground. Air and ground conductivity effects are not included, so there are no return currents, and air chemistry is treated simply by including attenuation terms for the gamma-ray and electron fluxes. Since the model does not contain as much detailed physics and chemistry as the sophisticated computer models developed for the study of geomagnetic turning effects, we have normalized our model to match the peak electron current given by such models at a distance of 500 m from the source.

We find that the fields produced by the ground asymmetry have a strong angular dependence. Directly above the burst point there is no EMP from this effect at all, and for viewing angles out to about 10° from vertical, the signal is weaker than the geomagnetic turning signal and therefore of little interest. For viewing angles larger than 10°, the signal strength grows rapidly so that for angles of 30° and larger the signal is much stronger than that from the magnetic effect. At 75° from vertical the power radiated from a surface burst by this effect is over 50 times that produced by geomagnetic turning. The shape of the pulse is also angle dependent; the large-angle pulses have a slightly faster risetime and a more bipolar shape than do the small-angle pulses. It is possible this angular dependence may explain some anomalies seen in satellite observations of EMP.

The present calculation attempts to model the complex mechanism by which surface bursts generate EMP. The results of this model indicate that the signal produced is comparable with or greater than that produced by geomagnetic turning, and we therefore intend to pursue a more detailed calculation of the effect.

We shall work in cgs units in this report unless stated otherwise.

II. GEOMETRY OF THE PROBLEM

Consider an explosion taking place near the earth's surface. We shall take the location of the explosion as the origin of a spherical coordinate system, with the $\theta = 0$ direction being radially outward from the earth. We shall observe the explosion from a remote point $\vec{R}$ with coordinates

$$\vec{R} = R(\sin\theta\cos\phi, \sin\theta\sin\phi, \cos\theta). \tag{2.1}$$

We shall then define a polar angle ψ and an azimuthal angle ζ relative to $\vec{R}$ (see Fig. 1). The location of a second point $\vec{r}$ is given in terms of these angles by

$$\vec{r} = r \begin{pmatrix} \cos\theta\cos\phi\sin\psi\cos\zeta & + & \sin\theta\cos\phi\cos\psi & - & \sin\phi\sin\psi\sin\zeta \\ \cos\theta\sin\phi\sin\psi\cos\zeta & + & \sin\theta\sin\phi\cos\psi & + & \cos\phi\sin\psi\sin\zeta \\ \cos\theta\cos\psi & & - \sin\theta\sin\psi\cos\zeta & & \end{pmatrix}. \tag{2.2}$$

The distance between the points is

$$\left|\vec{R} - \vec{r}\right| = \sqrt{R^2 + r^2 - 2Rr\cos\psi}. \tag{2.3}$$

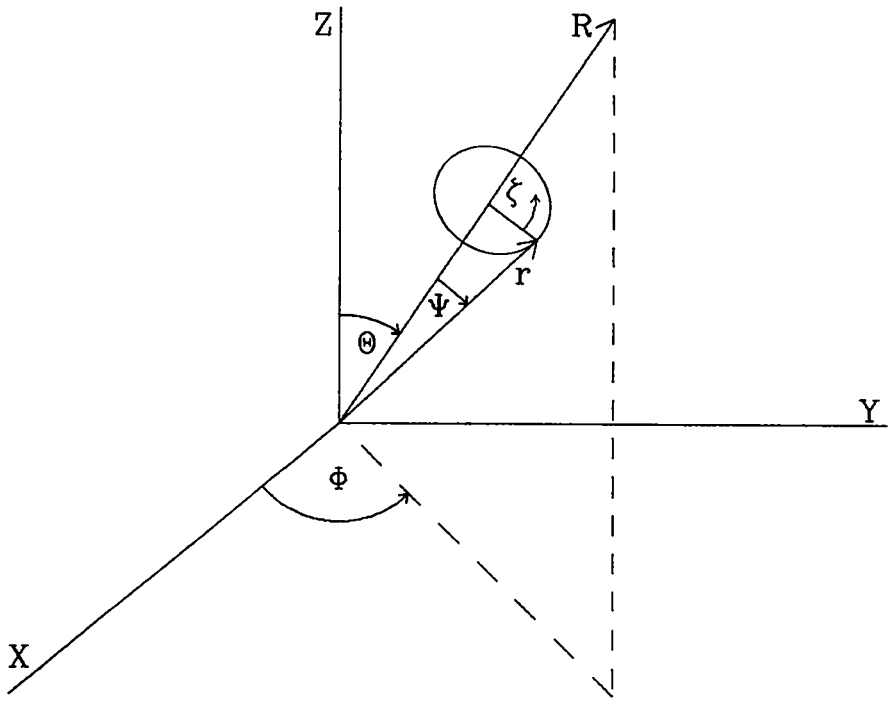

Fig. 1. Geometry of the model.

III. RADIATION FROM A VOLUME ELEMENT

The electromagnetic radiation fields seen at point $\vec{R}$ due to a time-changing current density $\vec{j}$ in a volume element dV located at point $\vec{r}$ are given by

$$d\vec{E} = \frac{1}{c^2}\left[\frac{\hat{n}\times(\hat{n}\times\dot{\vec{j}})}{\left|\vec{R}-\vec{r}\right|}\right]_{ret} dV \tag{3.1}$$

and

$$d\vec{B} = \hat{n}\times d\vec{E}, \tag{3.2}$$

where

$$\dot{\vec{j}} = \frac{d\vec{j}}{dt}, \quad \hat{n} = \frac{\vec{R}-\vec{r}}{\left|\vec{R}-\vec{r}\right|}, \text{ and } t_{ret} = t - \frac{\left|\vec{R}-\vec{r}\right|}{c}. \tag{3.3}$$

The subscript on the right-hand side of Eq. (3.1) means that the quantities inside the brackets are to be evaluated at the retarded time given in Eq. (3.3). $\hat{n}$ is a unit vector in the direction of $\vec{R}-\vec{r}$, and c is the speed of light.

We shall assume the currents are purely radial, so $\vec{r}$ and $\vec{j}$ are parallel to each other. Using Eqs. (2.1) and (2.2) we find

$$\hat{n} = \frac{1}{\left|\vec{R} - \vec{r}\right|} \begin{pmatrix} s_\theta c_\phi (R - r c_\psi) & - r c_\theta c_\phi s_\psi c_\zeta & + r s_\phi s_\psi s_\zeta \\ s_\theta c_\phi (R - r c_\psi) & - r c_\theta s_\phi s_\psi c_\zeta & - r s_\phi s_\psi s_\zeta \\ c_\theta (R - r c_\psi) & + r s_\theta s_\psi c_\zeta & \end{pmatrix}, \tag{3.4}$$

$$\hat{n} \times \dot{\vec{j}} = \frac{R\dot{j}}{\left|\vec{R} - \vec{r}\right|} \begin{pmatrix} -c_\theta c_\phi s_\psi s_\zeta & - s_\phi s_\psi c_\zeta \\ -c_\theta s_\phi s_\psi s_\zeta & + c_\phi s_\psi c_\zeta \\ s_\theta s_\psi s_\zeta & \end{pmatrix}, \tag{3.5}$$

and

$$\hat{n} \times (\hat{n} \times \dot{\vec{j}}) = \tag{3.6}$$

$$\frac{-R\dot{j}}{\left|\vec{R} - \vec{r}\right|} \begin{pmatrix} R s_\psi (c_\theta c_\phi c_\zeta - s_\phi s_\zeta) & + r(-c_\theta c_\phi s_\psi c_\psi c_\zeta & + s_\phi s_\psi c_\psi s_\zeta + s_\theta c_\phi s_\psi^2) \\ R s_\psi (c_\theta s_\phi c_\zeta - c_\phi s_\zeta) & + r(-c_\theta s_\phi s_\psi c_\psi c_\zeta & - c_\phi s_\psi c_\psi s_\zeta + s_\theta s_\phi s_\psi^2) \\ -R s_\theta s_\psi c_\zeta & + r(s_\theta c_\psi s_\psi c_\zeta & + c_\theta s_\psi^2) \end{pmatrix},$$

where $s_\theta = \sin\theta$, $c_\theta = \cos\theta$, etc. The gamma-ray mean free path is on the order of a hundred meters at sea level, and all of the Compton currents will be produced within a few mean free paths of the source. We are interested in the signal seen at a remote observation point hundreds or thousands of kilometers away from the burst, so for our purposes it is an excellent approximation to expand the expression for the electric field in terms of R/r and keep only the lowest order term. We find

$$d\vec{E} = \frac{-\sin\psi}{c^2 R} \left[j(c_\theta c_\phi c_\zeta - s_\phi s_\zeta,\ c_\theta s_\phi c_\zeta + c_\phi s_\zeta,\ -s_\theta c_\zeta) \right]_{ret} dV \tag{3.7}$$

and

$$t_{ret} = t - \frac{R}{c} + \frac{r\cos\psi}{c}. \tag{3.8}$$

To get the total radiation field seen at point $\vec{R}$ we must integrate over the entire region where $\vec{j}$ is significant. For a symmetric source the integral of Eq. (3.7) over ζ gives zero and there is no radiation, and for this reason the effect is not important for high-altitude explosions. For bursts near the surface, the range of ζ is restricted by the presence of the ground, and the integral is nonzero.

We shall consider an isotropic source of gamma rays and will take the ground into account by considering only those gamma rays with $z > -h$, where h is the height of the burst point above the ground. Any gamma rays that hit the ground are considered lost and do not produce any further currents. From Eq. (2.2) we see this implies the condition

$$r(\cos\theta\cos\psi - \sin\theta\sin\psi\cos\zeta) \geq -h. \tag{3.9}$$

For $r < h$ no gamma rays have hit the ground and the source is symmetric, so there is no radiation. For $r > h$ we may define

$$\psi_1 = \cos^{-1}\left(-\frac{h}{r}\cos\theta + \sqrt{1-\frac{h}{r}}\sin\theta\right) \tag{3.10}$$

and

$$\psi_2 = \cos^{-1}\left(-\frac{h}{r}\cos\theta - \sqrt{1-\frac{h}{r}}\sin\theta\right). \tag{3.11}$$

For $\psi > \psi_2$ all the gamma rays have hit the ground and no current density is produced, while for $\psi < \psi_1$ Eq. (3.9) is satisfied for any value of ζ and so once again the unrestricted integral over ζ yields zero. The interesting regime is when $\psi_1 \leq \psi \leq \psi_2$, and in this case we may rearrange Eq. (3.9) to give a condition on ζ:

$$\zeta_{min} < \zeta < 2\pi - \zeta_{min}, \quad \zeta_{min} = \cos^{-1}\left(\frac{\cos\theta\cos\psi - h/r}{\sin\theta\sin\psi}\right). \tag{3.12}$$

Integrating Eq. (3.7) over ζ then gives

$$d\vec{E} = \frac{2\sin\zeta_{min}\sin\psi}{c^2 R}\left[j(\cos\theta\cos\phi,\ \cos\theta\sin\phi,\ -\sin\theta)\right]_{ret} r^2 dr\sin\psi d\psi. \tag{3.13}$$

To make the problem more tractable analytically, we shall restrict ourselves to the case $h = 0$ in the remainder of this report. Equations (3.10), (3.11), and (3.12) then simplify to yield

$$\psi_1 = \pi/2 - \theta,\ \psi_2 = \pi/2 + \theta,\ \sin\zeta_{min} = \frac{\sqrt{\sin^2\theta - \cos^2\psi}}{\sin\theta\sin\psi}. \tag{3.14}$$

IV. CURRENT DENSITY

In the previous section we developed a formula for the far-field electromagnetic radiation produced by a given current distribution. To proceed with our EMP calculation we need a model for the current density j. We shall consider a point source of gamma rays that emits them isotropically and whose strength is characterized by the emission rate

$$\dot{\gamma}(t) = N(e^{-at} - e^{-bt}). \tag{4.1}$$

The gamma rays typically have energies in the range from 1.5 to 2 MeV. They will propagate through the atmosphere and eventually undergo Compton collisions, producing relativistic electrons with energies on the order of 1 MeV. The collision rate for this process will be denoted ν_g. The flux of gamma rays at radius r from the source is then given by

$$\Phi(r,t) = \frac{N\exp(-\nu_g r/c)}{4\pi R^2}\{\exp[-a(t-r/c)] - \exp[-b(t-r/c)]\}. \tag{4.2}$$

The current density produced per unit time is

$$\frac{\partial \jmath}{\partial t} = -\nu_g e \beta \Phi, \tag{4.3}$$

where $c\beta$ is the average radial velocity of the electrons.

The Compton electrons produced by the gamma rays will move outward from the source and undergo many collisions with the air molecules, bringing the electrons to a stop within a few meters of where they were created. Although the individual electrons will follow convoluted paths, the net current will be purely radial. We shall treat the electrons as having a constant β of 0.67 until they stop and shall include the effects of scattering by reducing the mean free path by a factor of 3/2, which is roughly the cosine of the average scattering angle. The electron collision rate will be denoted ν_e.

The total current density in a volume element at radius r is the sum of the current density produced locally by the scattering of the gamma rays and the currents transported in and out of the volume element. It satisfies the conservation equation

$$\frac{d\jmath}{dt} = \frac{\partial \jmath}{\partial t} - \nu_e \jmath - \frac{\beta}{r^2}\frac{\partial (r^2 \jmath)}{\partial r} \tag{4.4}$$

with the boundary condition

$$\jmath(t = r/c) = 0. \tag{4.5}$$

The solution of this equation is

$$\jmath = \frac{e\nu_g \beta N e^{-\nu_g r/c}}{4\pi r^2}\left(\frac{e^{-b(t-r/c)} - e^{(\nu_e - \beta\nu_g)(t-r/c)/(1-\beta)}}{\nu_e - \beta\nu_g - (1-\beta)b} - \frac{e^{-a(t-r/c)} - e^{-(\nu_e - \beta\nu_g)(t-r/c)/(1-\beta)}}{\nu_e - \beta\nu_g - (1-\beta)a}\right). \tag{4.6}$$

As mentioned in the Introduction, this model does not contain as much detailed air chemistry as the computer models developed for calculating the EMP due to geomagnetic turning. Although the source of the signal in our calculation is quite different, the current strengths should be the same in both cases, and so we have normalized our expression for the current to agree with the current calculated by existing computer codes at a distance of 500 m from the source. The source used was a 100-kt explosion with 0.1% of the energy emitted as gamma rays and a gamma-ray emission rate as given in Eq. (4.1) above. In the remainder of this report, we shall use the following hypothetical values of the parameters for a sample problem:

$$\begin{aligned} a &= 8.0 \times 10^7 \text{ /s} \\ b &= 1.0 \times 10^8 \text{ /s} \\ \nu_g &= 2.5 \times 10^6 \text{ /s} \\ \nu_e &= 3.0 \times 10^8 \text{ /s} \\ N &= 1.25 \times 10^{28} \text{ gammas/s} \end{aligned} \tag{4.7}$$

V. CALCULATION OF THE FIELD

Now that we have a model for the current density produced by the explosion, we may integrate Eq. (3.7) over the source region to obtain the electric field seen at a distant point. The limits of the angular integration are given in Eq. (3.14), while the limits of the radial integration are determined by the requirement that the retarded time must be positive. The expression for the electric field is then

$$|E| = \frac{e\nu_g\beta N}{2\pi Rc^2 \sin\theta} \int_{-\sin\theta}^{\sin\theta} d\mu \int_0^{\frac{cr}{1-\mu}} dr \left\{ \frac{ae^{-a(\tau-(1-\mu)r/c)} - \hat{\nu}e^{-\hat{\nu}(\tau-(1-\mu)r/c)/(1-\beta)}/(1-\beta)}{\hat{\nu}-(1-\beta)a} \right. \tag{5.1}$$

$$\left. - \frac{be^{-b(\tau-(1-\mu)r/c)} - \hat{\nu}e^{-\hat{\nu}(\tau-(1-\mu)r/c)/(1-\beta)}/(1-\beta)}{\hat{\nu}-(1-\beta)b} \right\} e^{-\nu_g r/c}\sqrt{\sin^2\theta-\mu^2},$$

where $\hat{\nu} = \nu_e - \beta\nu_g$, $\mu = \cos\psi$, and $\tau = t - R/c$.

The integral over r may be done analytically, and we find

$$|E| = \frac{e\nu_g\beta N}{2\pi Rc^2 \sin\theta} \int_{-\sin\theta}^{\sin\theta} d\mu \sqrt{\sin^2\theta-\mu^2} \left\{ \frac{e^{-\nu_g\tau/(1-\mu)} - e^{-a\tau}}{(1-\mu-\nu_g/a)(\hat{\nu}-(1-\beta)a)} \right.$$

$$- \frac{e^{-\nu_g\tau/(1-\mu)} - e^{-\hat{\nu}\tau/(1-\beta)}}{(1-\mu-(1-\beta)\nu_g/\hat{\nu})(\hat{\nu}-(1-\beta)a)}$$

$$\left. - \frac{e^{-\nu_g\tau/(1-\mu)} - e^{-b\tau}}{(1-\mu-\nu_g/b)(\hat{\nu}-(1-\beta)b)} + \frac{e^{-\nu_g\tau/(1-\mu)} - e^{-\hat{\nu}\tau/(1-\beta)}}{(1-\mu-(1-\beta)\nu_g/\hat{\nu})(\hat{\nu}-(1-\beta)b)} \right\} \tag{5.2}$$

The remaining integral over μ cannot be done in closed form and must be evaluated numerically. The results are fitted very well by the function

$$E(\tau,R,\theta) = \frac{A\exp(-\alpha\tau) - B\exp(-\beta\tau) + (B-A)\exp(-\gamma\tau)}{R}, \tag{5.3}$$

where $\gamma = \beta - (b-a)$. To determine the parameters for the fit we first observe that its late-time behavior is controlled by the first term on the right-hand side of Eq. (5.3), and so A and α can be found by a least-squares fit to the late-time values of the integral. Once these are known we fix B by requiring the peak values of the integral and the fit to match. β is then found by a least-squares fit to the values of the integral over the entire length of the pulse. The integrals and fits for our sample problem viewed from geosynchronous orbit ($R = 4.22 \times 10^9$ cm) and various angles of observation are shown in Figs. 2 through 6, and the fit parameters are given in Table I. The fit coefficients are given reasonably well by the following formulae:

$$
\begin{aligned}
A &= 177.0 + 10.3\theta + 0.73\theta^2 \text{ esu/cm} \\
B &= 1.04(4) + 4.23(3)\theta + 26.2\theta^2 \text{ esu/cm} \\
\alpha &= 2.48(6)\exp[8.54(-4)\theta + 1.48(-4)\theta^2] \text{ Hz} \\
\beta &= 7.69(7)\exp[-1.59(-3)\theta + 2.69(-5)\theta^2] \text{ Hz},
\end{aligned} \tag{5.4}
$$

where θ is in degrees.

The electric field starts off negative and reaches a maximum amplitude E_1 at time t_1, which is about the same time as $\dot{\gamma}$ peaks. The field then decreases fairly rapidly, passes through zero, and reaches a second, smaller positive peak value E_2 at time t_2. After this point it decays slowly to zero. The strength of the field increases as the viewing angle becomes larger. The pulse shape is also a function of angle, with the large-angle pulses having a larger positive component at late times and a slightly faster risetime. Table II gives the values of the field at the first and second maxima for an observation point in geosynchronous orbit and the times at which these occur.

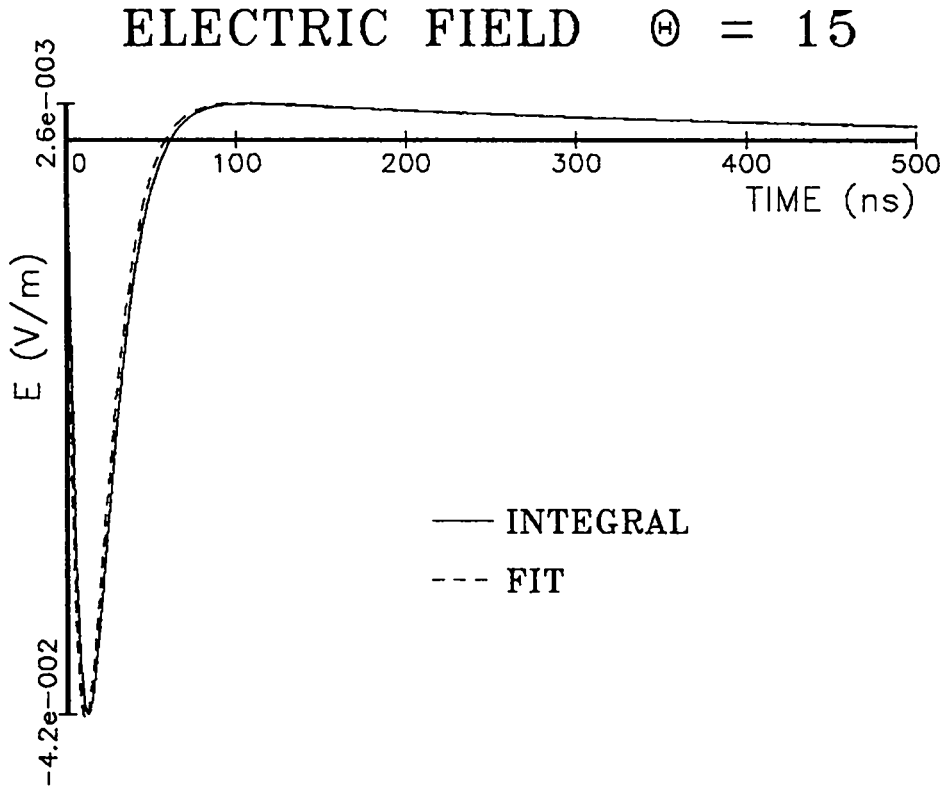

Fig. 2. Electric field at 15°.

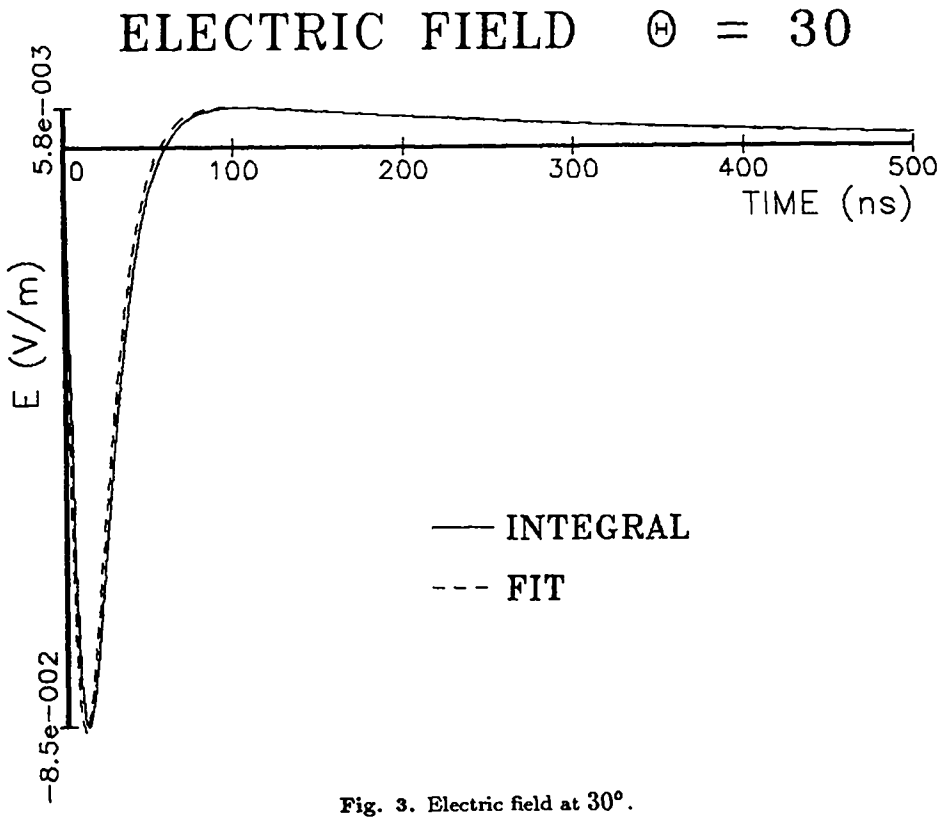

Fig. 3. Electric field at 30°.

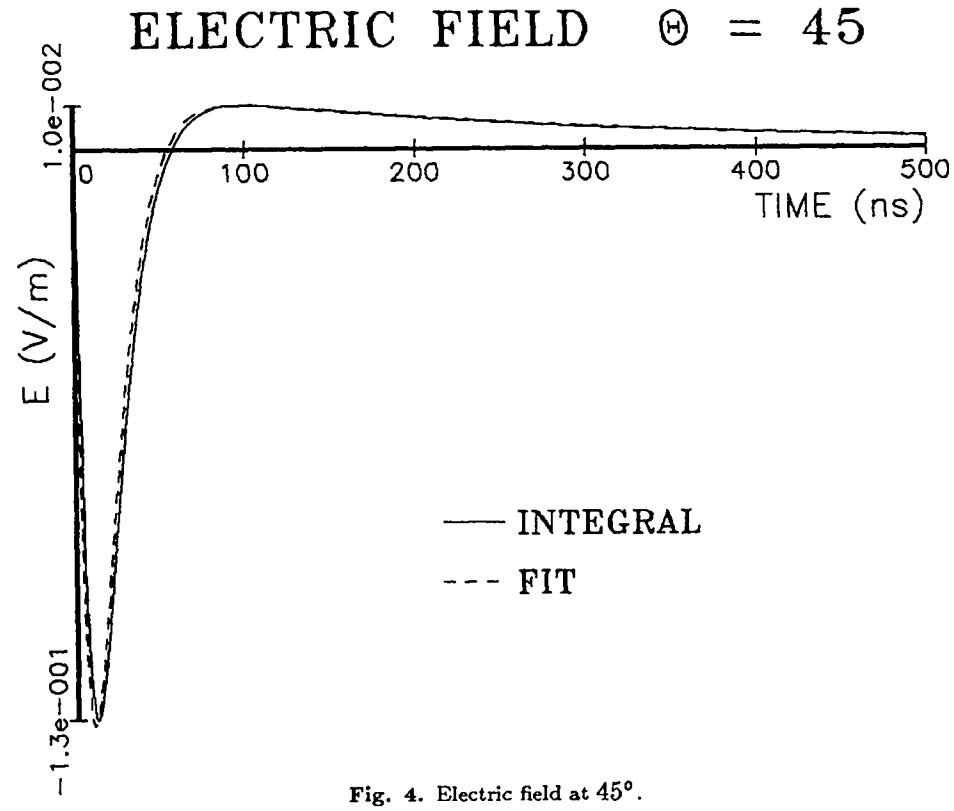

Fig. 4. Electric field at 45°.

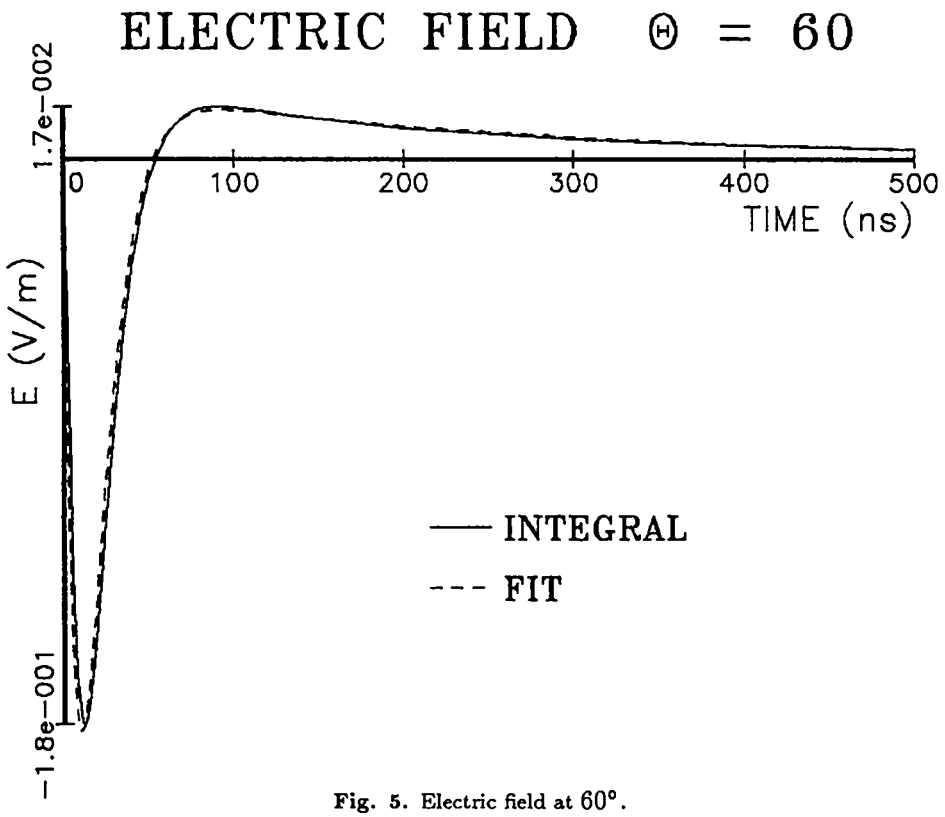

Fig. 5. Electric field at 60°.

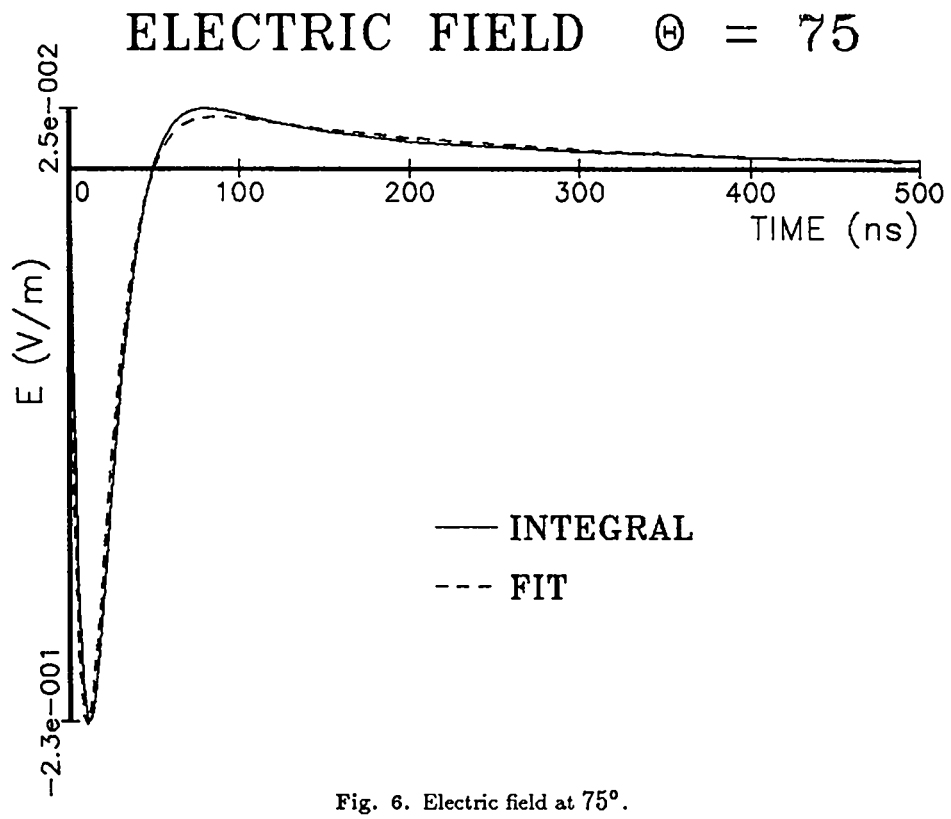

Fig. 6. Electric field at 75°.

TABLE I. Electric Field Fit Parameters

Angle	A	B	α	β
15°	5.05(2)	7.92(4)	2.59(6)	7.53(7)
30°	1.14(3)	1.62(5)	2.91(6)	7.54(7)
45°	2.07(3)	2.53(5)	3.52(6)	7.57(7)
60°	3.49(3)	3.58(5)	4.38(6)	7.64(7)
75°	5.03(3)	4.75(5)	5.13(6)	7.96(7)

Where n.nn(p) stands for n.nn $\times$ 10^p.

TABLE II. Electric Field Maxima at $R = 4.22 \times 10^9$ cm

Angle	E_1 (V/m)	t_1 (ns)	E_2 (V/m)	t_2 (ns)
15°	-0.42	12	0.026	110
30°	-0.85	12	0.058	105
45°	-1.31	12	0.101	100
60°	-1.80	11.5	0.167	93
75°	-2.32	11.5	0.251	80

VI. FREQUENCY SPECTRUM

We now have the electric field as a function of time, but the quantity of interest to most observers is the energy incident on a receiver as a function of frequency. To find the energy we first need the Fourier transform of the electric field, given by

$$E(\omega) = \frac{1}{\sqrt{2\pi}} \int_{-\infty}^{\infty} e^{i\omega t} E(t) dt. \tag{6.1}$$

For the functional form given in Eq. (5.3) we have

$$E(\omega) = \left[\frac{A(\alpha + i\omega)}{\alpha^2 + \omega^2} - \frac{B(\beta + i\omega)}{\beta^2 + \omega^2} + \frac{(B - A)(\gamma + i\omega)}{\gamma^2 + \omega^2} \right] \frac{1}{R}. \tag{6.2}$$

The energy density in frequency space is then

$$\mathcal{E} = \frac{c}{2\pi R^2}\left[\frac{A^2}{\alpha^2+\omega^2} + \frac{B^2}{\beta^2+\omega^2} + \frac{(B-A)^2}{\gamma^2+\omega^2} - \frac{2AB(\alpha\beta+\omega^2)}{(\alpha^2+\omega^2)(\beta^2+\omega^2)}\right.$$

$$\left. + \frac{2A(B-A)(\alpha\gamma+\omega^2)}{(\alpha^2+\omega^2)(\gamma^2+\omega^2)} - \frac{2B(B-A)(\beta\gamma+\omega^2)}{(\beta^2+\omega^2)(\gamma^2+\omega^2)}\right]. \tag{6.3}$$

Figure 7 shows this function for our sample problem at $R = 4.22 \times 10^9$ cm (geosynchronous orbit) and an angle of 60°.

The energy emitted in a particular frequency band is given by

$$I(\omega_1,\omega_2) = \frac{c}{2\pi R^2}\left\{T(\alpha)\left[\frac{A^2}{\alpha} - \frac{2AB}{\alpha+\beta} + \frac{2A(B-A)}{\alpha+\gamma}\right]\right.$$

$$\left. + T(\beta)\left[\frac{B^2}{\beta} + \frac{2AB}{\alpha+\beta} - \frac{2B(B-A)}{\beta+\gamma}\right] + T(\gamma)\left[\frac{(B-A)^2}{\gamma} + \frac{2A(B-A)}{\alpha+\gamma} - \frac{2B(B-A)}{\beta+\gamma}\right]\right\}, \tag{6.4}$$

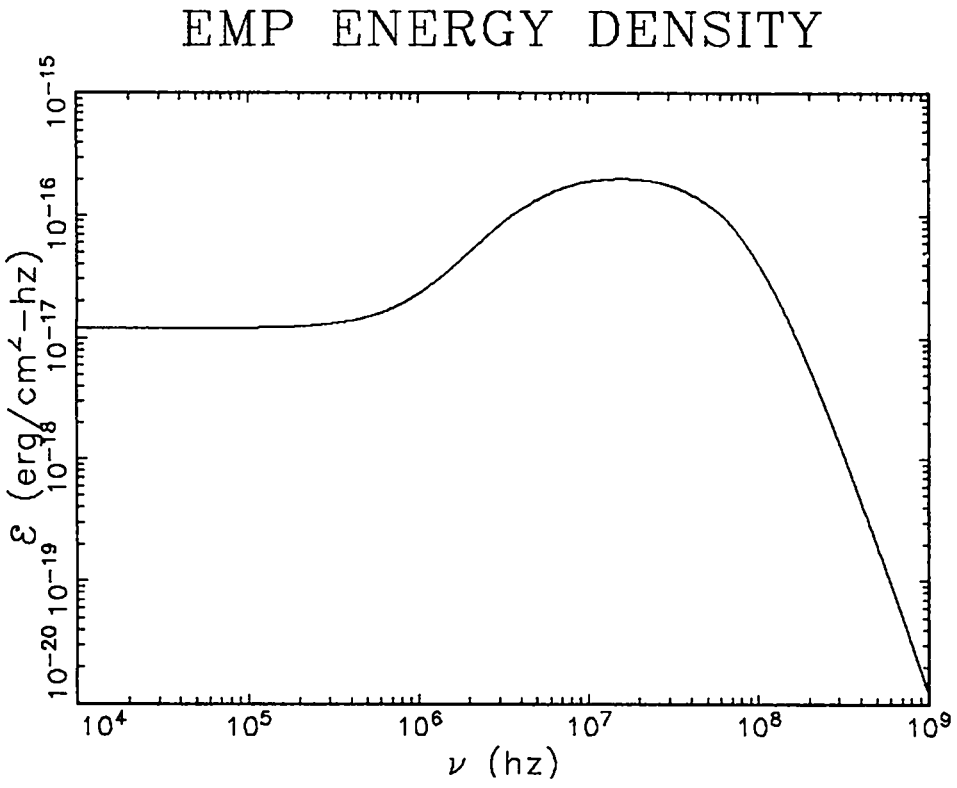

Fig. 7. Energy density at 60°.

where

$$T(\alpha) = \tan^{-1}(\omega_2/\alpha) - \tan^{-1}(\omega_1/\alpha) \tag{6.5}$$

and ω_1, ω_2 are the lower and upper edges of the frequency band.

Our calculation is more accurate for high-frequency radiation, since this component of the radiation comes from the early part of the gamma-ray pulse and is produced before air and ground conductivity effects have time to develop. Let us consider the energy emitted in a 1-MHz bandwidth at frequencies of 50, 100, 150, and 200 MHz. The results for our sample problem viewed from geosynchronous orbit and seen from an angle of 60° are given in Table III. The energy density is given in terms of ergs/cm^2. (To convert to joules/m^2 divide by 10^3.) These energy densities are about a factor of 10 greater than those calculated for the geomagnetic turning EMP. Given the degree of uncertainty in both calculations this number should not be taken too seriously, but we believe it shows this effect is potentially important and deserves further study.

ACKNOWLEDGMENTS

I would like to thank Bob Massey for many helpful discussions of this problem and Bill Clodius for pointing out an error in the calculation.

TABLE III. Energy Density at $R = 4.22 \times 10^9$ cm

Angle	50 MHz	100 MHz	150 MHz	200 MHz
15°	2.85(-12)	6.75(-13)	2.96(-13)	1.66(-13)
30°	1.29(-11)	3.08(-12)	1.35(-12)	7.59(-13)
45°	3.59(-11)	8.69(-12)	3.83(-12)	2.15(-12)
60°	7.88(-11)	1.93(-11)	8.57(-12)	4.81(-12)
75°	1.55(-10)	3.85(-11)	1.70(-11)	9.58(-12)

Printed in the United States of America
Available from
National Technical Information Service
US Department of Commerce
5285 Port Royal Road
Springfield, VA 22161

Microfiche (A01)

Page Range	NTIS Price Code	Page Range	NTIS Price Code	Page Range	NTIS Price Code	Page Range	NTIS Price Code
001-025	A02	151-175	A08	301-325	A14	451-475	A20
026-050	A03	176-200	A09	326-350	A15	476-500	A21
051-075	A04	201-225	A10	351-375	A16	501-525	A22
076-100	A05	226-250	A11	376-400	A17	526-550	A23
101-125	A06	251-275	A12	401-425	A18	551-575	A24
126-150	A07	276-300	A13	426-450	A19	576-600	A25
						601-up*	A99

*Contact NTIS for a price quote.

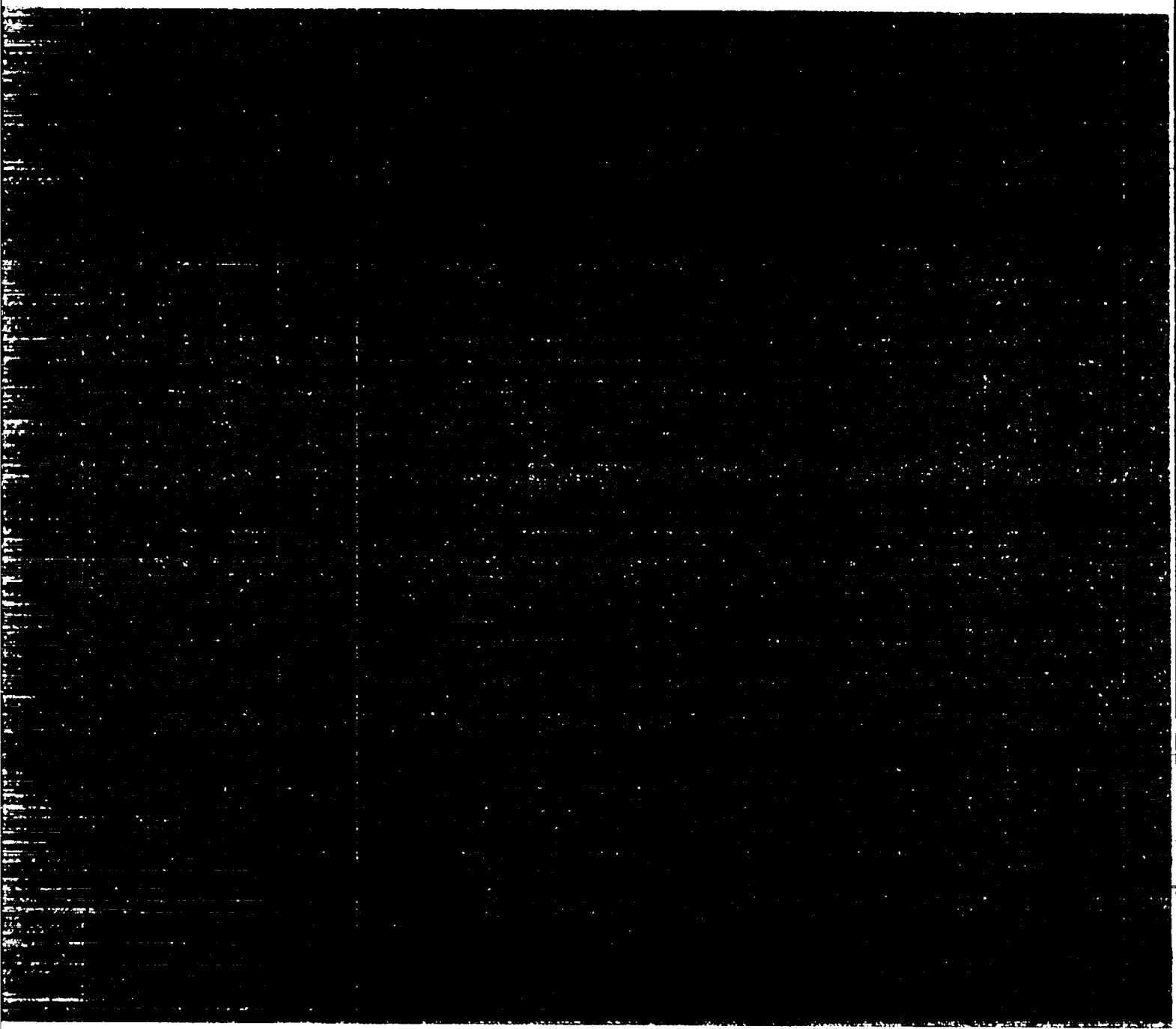

Los Alamos